

Role of Data-driven Regional Growth Model in Shaping Brain Folding Patterns

Jixin Hou¹, Zhengwang Wu², Xianyan Chen³, Li Wang², Dajiang Zhu⁴, Tianming Liu⁵, Gang Li^{2*},
Xianqiao Wang^{1*}

¹School of Environmental, Civil, Agricultural and Mechanical Engineering, College of Engineering, University of Georgia, Athens, GA 30602, USA

²Department of Radiology and Biomedical Research Imaging Center, The University of North Carolina at Chapel Hill, NC 27599, USA

³Department of Epidemiology and Biostatistics, College of Public Health, University of Georgia, Athens, GA 30602, USA

⁴Department of Computer Science and Engineering, The University of Texas at Arlington, Arlington, TX 76019, USA

⁵School of Computing, The University of Georgia, Athens, GA 30602, USA

*Corresponding Author: gang_li@med.unc.edu, xqwang@uga.edu

Table S1: Model parameters used in the cortical folding simulations.

Parameter	Value	Units	Description
ρ_{gray}	1.05	g/cm^3	Density of gray matter
ρ_{white}	1.02	g/cm^3	density of white matter
E_{gray}	0.31	kPa	Elastic modulus for gray matter
E_{white}	0.45	kPa	Elastic modulus for white matter
K_{gray}	5.17	kPa	Bulk modulus for gray matter
K_{white}	7.50	kPa	Bulk modulus for white matter
ν	0.49	--	Poisson's ratio for gray and white matter
c	0.02	--	Damping coefficient for viscous damping

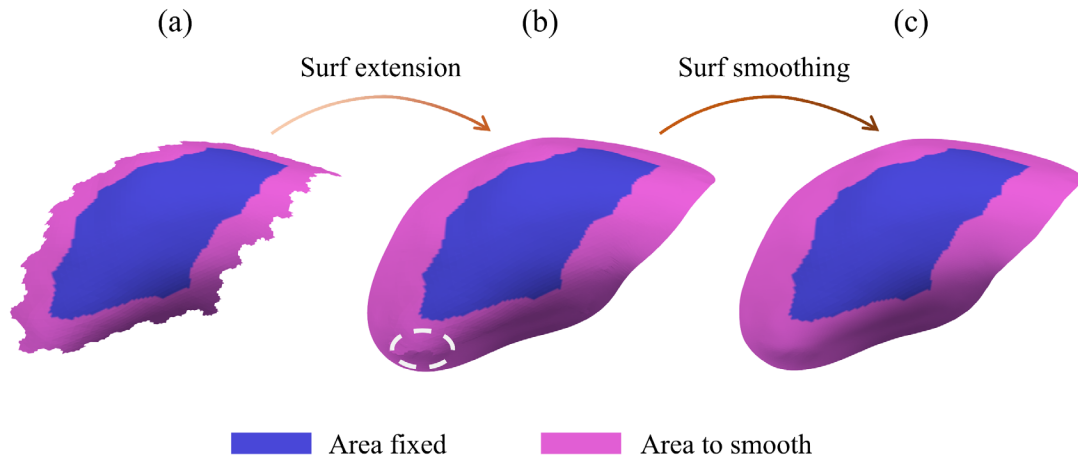


Figure S1. Boundary smoothing procedure. Illustration of boundary smoothing using an example of region 4. (a) Extracted surface from the brain model with zigzag boundary, unsmoothed area is determined when the distances between vertices and their nearest boundary are greater than 2mm; (b) Surface extension along the local curvature to remove the zigzag boundary; (c) Smoothing performed for area (pink color) near the boundary. Blue area remains unchanged during the extension and smoothing process. Inset shows the bumpy area before smoothing.

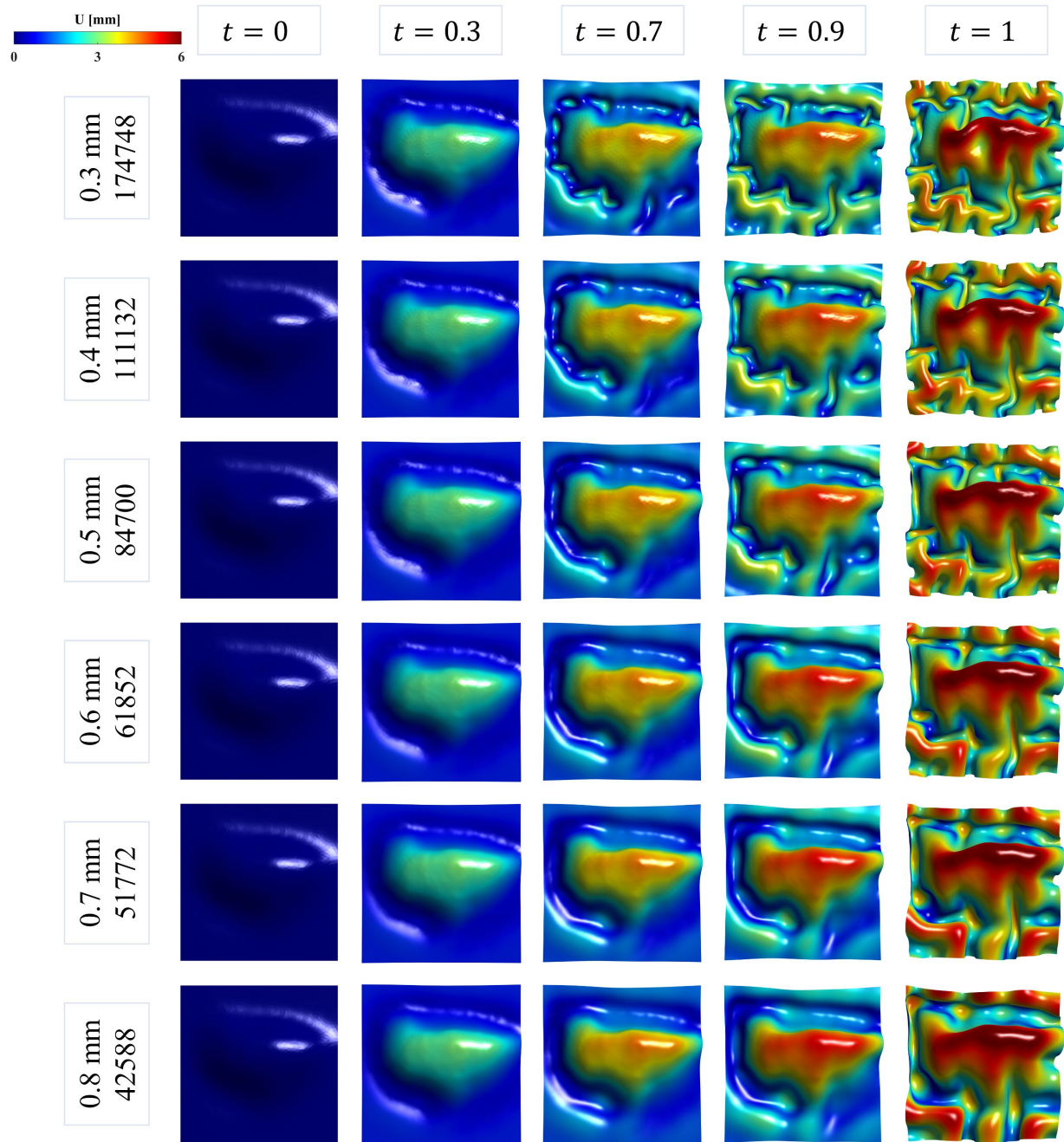


Figure S2. Qualitative mesh sensitivity analysis. Longitudinal folding patterns for region 1 using various mesh densities. The average mesh size and corresponding mesh numbers for the cortex part are displayed on the left. An isotropic growth model with constant growth ratio of $g = \sqrt{8}$ is used.

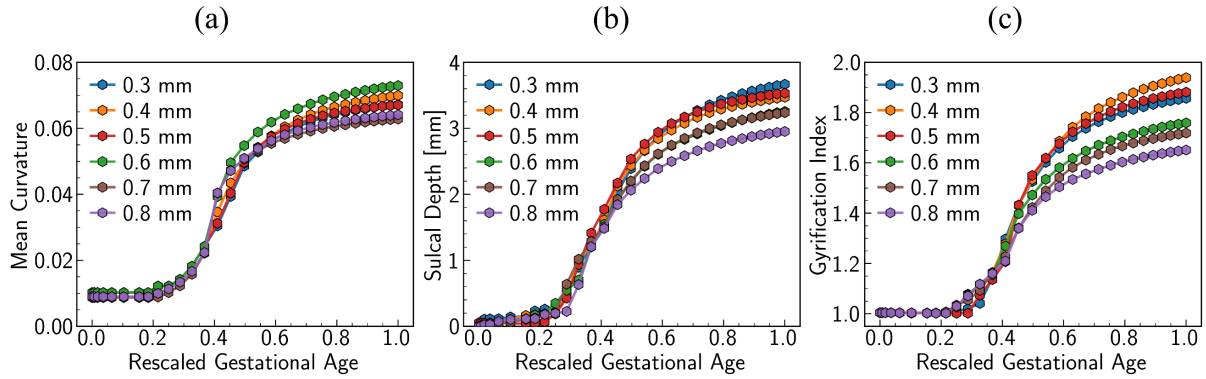


Figure S3. Quantitative mesh sensitivity analysis. Comparison of Mean curvature (a), sulcal depth (b), and gyrfication index (c) for simulated brain models with various mesh densities. Mean curvature is determined by averaging absolute dimensionless mean curvature at each point.

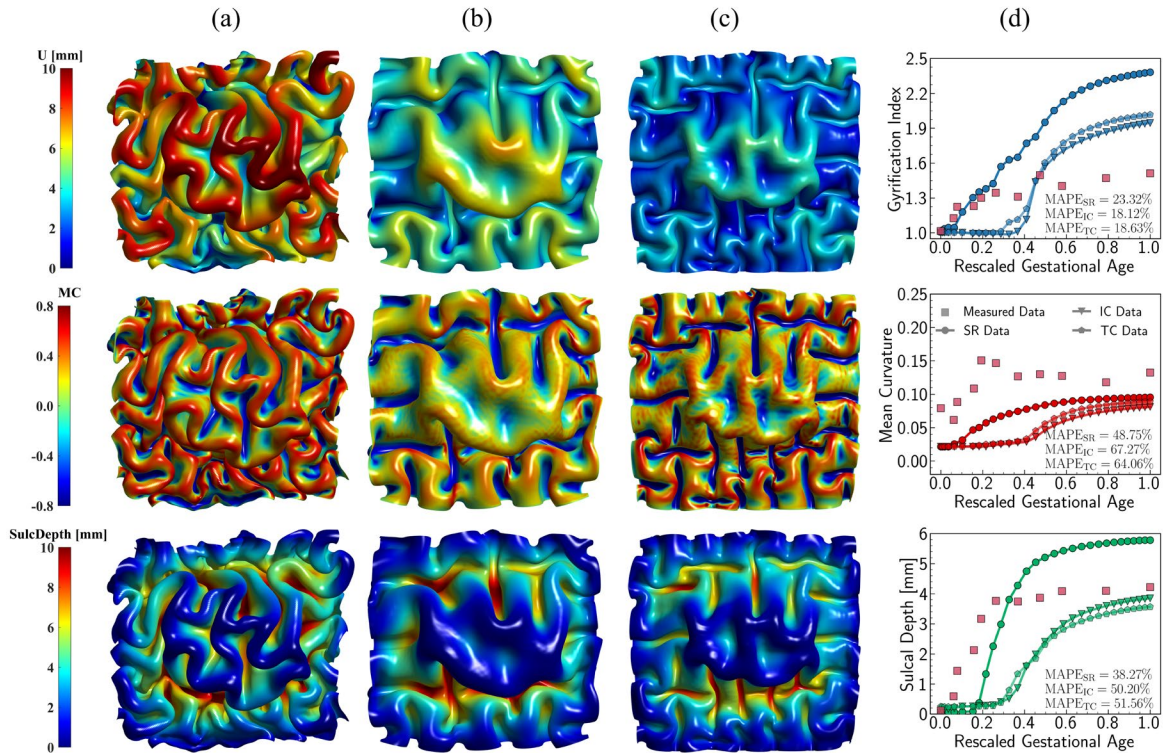


Figure S4. Symbolic regression growth model vs classic growth model. Impact of different growth models, including growth model predicted from symbolic regression (SR) algorithm (a), isotropic model with constant growth ratio (IC) model (b), and tangential model with constant growth rate (TC) (c), on modeling cortical folding patterns. Distributions of displacement (U), mean curvature (MC), and sulcal depth (SulcDepth) of region 16 are displayed with their quantitative measure present at the right (d). The simulation errors relative to real brain imaging data are quantified using MAPE. The growth ratio in both isotropic growth model is $g = \sqrt{8}$, while $g_t = \sqrt{8}$ in the tangential direction and no radial growth occurs for the pure tangential model, $g_r = 1$.